Hidden metallic object localization by using Giant Magnetic Resistor sensors

W. Renhart*, M. Bellina*, C. Magele * and A. Köstinger**

*Institute for Fundamentals and Theory in Electrical Engineering, Kopernikusgasse 24/3, A-8010 Graz, Austria
** Institute of Medical Engineering, Kronesgasse 5/II, A-8010 Graz, Austria
E-mail: werner.renhart@TUGraz.at

ABSTRACT

Purpose - The purpose of this paper is the achievement of a very acurate localization of hidden metallic objects in human medicine applications.

Design/methodology/approach - The proposed methodology takes advantage of the eddy current effect within a metallic object. Its magnetic reaction field will be measured, eg. with Giant Magnetic Resistor (GMR) sensors.

Findings - A comparison of measurements and numerical results obtained by finite element computations demonstrate the reliability and positively gives a clue about the feasibility of the suggested method.

Research limitations/implications - While measuring noisy signals the use of a lock-in amplifier is rather expensive. Especially, in applications with a high number of GMR sensors the use of channel multiplexer must be considered, which again may generate noise.

Practical implications - Appropriate shielding of external fields in the measurement setup ensures results of satisfying quality.

Keywords Eddy currents, Giant Magnetic Resistor, Hidden object localization, Signal to noise ratio.

Paper type Research paper

I. Introduction

In human medicine, a precise prediction of hidden objects like intra-medullary nails is required. In clinical life, the localization mostly will be done with the aid of X-ray radioscopic imaging. To overcome the drawback of a possible X-ray contamination, other methods are requested. In the proposed method, advantage will be taken of the eddy currents in the metallic object. These eddy currents are enforced by an external impressed time harmonic magnetic field. Its magnetic reaction field will be measured with a GMR sensor setup [Jen-Tzong *et al.* (2006)]. With the measurement data obtained, a prediction of the localization of the object should be possible. In order to gain information about the feasibility of the proposed method, a special view has to be cast on the noise behavior of the signal measurement. A comparison to results computed with the finite element method will demonstrate the accuracy of the results and increases its reliability. Thereby, the well known $\vec{A}v$-formulation [Bíró (1999)] has been employed.

II. Giant Magnetoresistive sensors

W. Thomson, better known as Lord Kelvin, discovered in 1856/57 the phenomenon of **magnetoresistance, (MR)** [Thomson (1856-1857)]. It is based on the influence of a magnetic field on the resistivity of an electrical conductor. As recently as in 1988, Peter Grünberg (Germany) and the French, Albert Fert independently found materials to capitalize this phenomenon which led to a substantial technical applicability. Therewith, the notation **giant magnetoresistance, (GMR)** has been established. In favor the Nobel Prize for physics has been awarded to them [Nobel (2007)].

Basically, the GMR sensor consists of at least three layers, as shown in Fig. 1. Two magnetically soft ferrite alloys are separated by an electric conductor, eg. Cu, of nanometric thickness. In case of the absence of an external magnetic field the ferrite layers are magnetizied in opposite direction. A quantum mechanical effect caused by the electron spins acts on the mean free path of the electrons which become short [Howson *et al.* (1999)]. As a consequence the electric resistivity becomes large (left side in Fig. 1). If the sensor is exposed to an external magnetic field, the magnetization of both ferrite layers becomes parallel (right side in Fig. 1). Due to the new electron spin situation, the mean free path of the electrons becomes larger, attending with a remarkable decrease of the electric resistance.

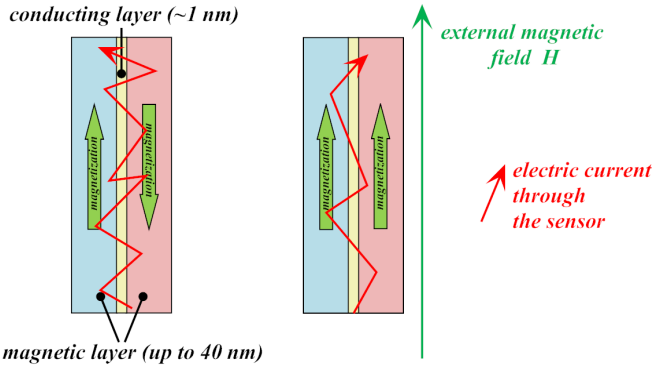

Fig. 1. Thin conducting layer sandwiched by two magnetic soft ferrite alloy layers, with and without external field, mean free path for electrons indicated.

Qualitatively, the percentual change in resistance $\Delta R/R_{min}$ is shown in Fig. 2.

The largest resistivity can be observed when the external field is zero, which corresponds to an antiparallel magneti-

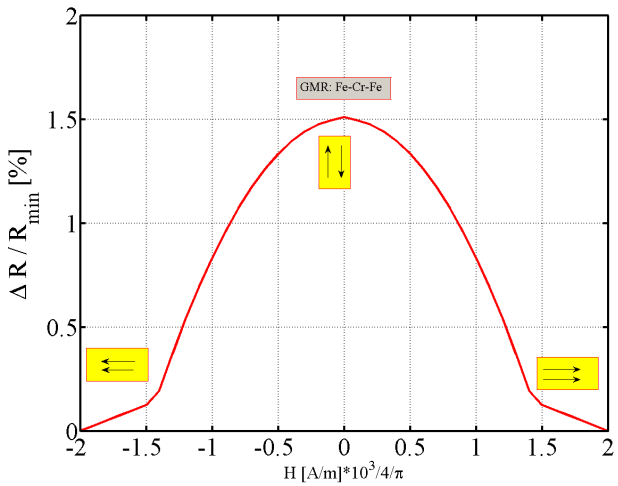

Fig. 2. Relative change of resistivity versus the external magnetic field.

zation of the ferrite layers. Out of the field free point the characteristic shows a symmetric behavior, independent of the parallel magnetization to be up or down. The decrease of the resistivity also may be influenced by the thickness of the conducting layer. The smaller this layer is manufactured, the larger the decrease of ΔR becomes. So, Fig. 2 shows a general behavior, only.

For magnetometric purposes the GMR sensor is designed as Wheatstone bridge. Thereby, two of the four resistors made of GMR-material are shielded, whereas the unshielded resistors lead to the field dependent imbalance of the bridge. Into an integrated circuit all bridge resistrors and the shielding components are built-in. Characteristic for such a field dependent sensor is its axis of sensitivity (Fig. 3). If the field to be measured is aligned parallel to this axis, a maximum sensor output voltage is implicated.

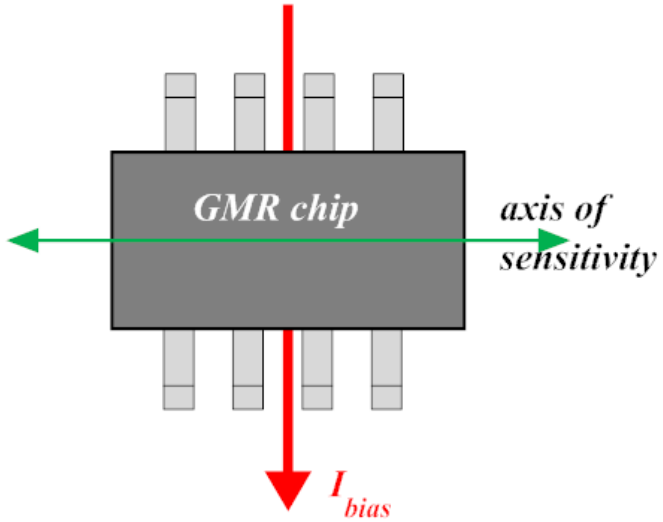

Fig. 3. Axis of sensitivity of an SOIC8 packaged sensor, bias current indicated.

Considering the voltage delivered by the sensor chip (Fig. 4), a linear devolution over a large range of the magnetic field is given. Nevertheless, the soft ferritic materials show a slight hysteretic behavior. For our application the induced eddy currents in the metallic object are very small. Hence the amplitudes to be measured will be small, as well. To increase the output voltage, a point of operation in the sensitivity characteristics can be adjusted with the aid of a direct current I_{bias}. In our measurement setup this kind of biasing has been accomplished by a current carrying conductor path on the back side of the printed circuit board where the sensor chip is mounted.

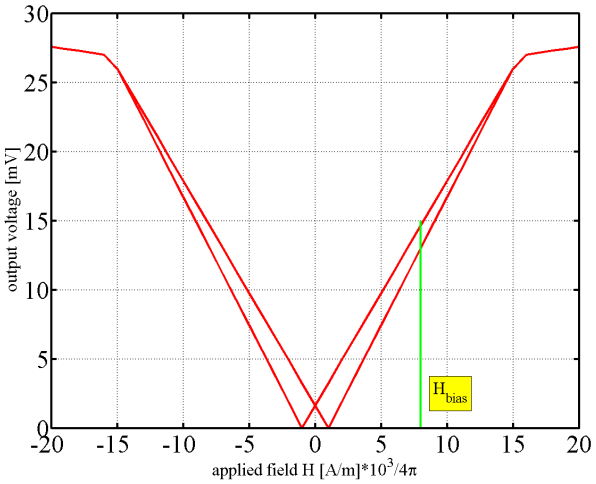

Fig. 4. Sensitivity characteristics of the sensor on the magnetic field.

III. Signal Measurement in Noisy Environment

Our measurement setup (Fig. 5) contains several sources of noise. In principal all voltage and current sources, the GMR sensor and the subsequent signal processing devices give cause for noise.

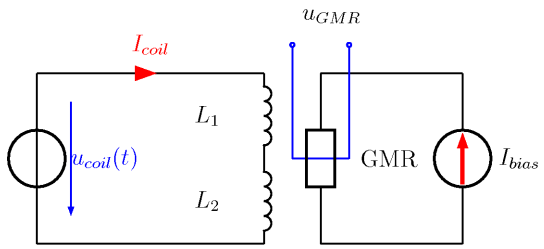

Fig. 5. General network circuit of the measurement setup in use.

A voltage source drives a timeharmonic current through the excitation coils that produces the magnetic field to generate eddy currents in a conducting specimen. This specimen is not drawn in Fig. 5. A frequency of 100 kHz has been selected in our work. Another source biases the GMR sensor with a

constant direct current I_{bias}. With u_{GMR} the output voltage of the sensor is termed. All together, a very noisy environment is given. Several researching work has been done to describe the noise behavior of GMR sensors. In [Nor *et al.*] the influence of the layer dimensions, especially length and width have been reported. Noise measurements and analyses of GMR sensors for low as well as for high frequency applications are described in the works of [Jury *et al.* (2002)]. Optimized GMR sensors with improved linearity behavior have been investigated by [Fermon *et al.* (2005)]. Following these results, two sources of noise have to be considered, mainly. Thermal noise in the resistor due to thermal forced fluctuations and another part depending on the inverse of the frequency f. Hence, a diligent treatment must be observed when taking the measurements.

A. Use of a lock-in amplifier

Very convenient but also expensive is the use of a lock-in amplifier to measure noise signals. The amplifier takes advantage of the orthogonality between a sine and a co-sine function. A schematic chart of its functionality is shown in Fig. 6.

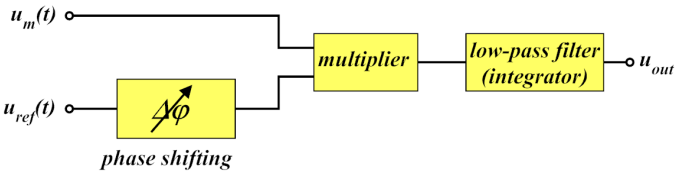

Fig. 6. Chart of a lock-in amplifier.

A multiplication of the measured signal with a reference signal and a subsequent integration with the aid of a low-pass filter cleans the signal from noise and improves the signal to noise ratio significantly.

Assuming that the signal $u_m(t)$ to be measured can be described by

$$u_m(t) = \sqrt{2}U_m \sin(\omega_m t + \varphi_m) \tag{1}$$

with ω_m as known angular frequency of the problem, a multiplication of this function with another timeharmonic function of the form

$$u_{ref}(t) = \sqrt{2}U_{ref} \sin(\omega_{ref} t + \varphi_{ref}) \tag{2}$$

at equal angular frequencies $\omega_m = \omega_{ref}$ leads to

$$\begin{aligned} u_m(t) \cdot u_{ref}(t) = U_m U_{ref}[\cos(\varphi_m - \varphi_{ref}) - \\ - \cos(2\omega_m t + \varphi_m + \varphi_{ref})]. \end{aligned} \tag{3}$$

The first term on the right hand side is independent on the time t, whereas the second one pulses with twice the measurement angular frequency. After an averaging over the cycle duration T

$$U_{out} = \frac{1}{T} \int_t^{t+T} u_m(\tau) \cdot u_{ref}(\tau)\, d\tau \tag{4}$$

the second term vanishes and therewith the noise in the output voltage, as well. With $\varphi_m - \varphi_{ref} = \Delta\varphi$ the voltage out of the lock-in amplifier becomes

$$U_{out}(DC) \sim \quad U_m U_{ref} \cos(\Delta\varphi). \tag{5}$$

This DC voltage only depends on the phase difference between the signal to be measured and the reference signal. The lock-in amplifier is also called phase sensitive detector.

B. Signal averaging

Further reduction of noise in the measurements can be achieved by a so called signal averaging. Instead of taking one set of measuring data only, the measurement procedure must be repeated N times. As outlined in [Kraftmaker (2010)] and [Umer and Sabieh (2006)], the signal to noise ratio then will be improved by the factor $\sqrt{N}$.

IV. Finite Element Formulation

In order to compare the measurements numerical computations have been done. Therefore, the well known $\vec{A}, v - \Phi$ formlation for eddy current problems [Bíró (1999)] has been applied. Derived from the Maxwell equations and its constitutive relations

$$\begin{aligned} &\nabla \times \vec{E} = -j\omega\vec{B}, \quad \nabla \times \vec{H} = \vec{J} \\ &\vec{J} = \sigma\vec{E}, \quad \vec{B} = \mu\vec{H} \end{aligned} \tag{6}$$

the potentials $\vec{A}$ and v can be introduced

$$\vec{B} = \nabla \times \vec{A}, \quad \vec{E} = -j\omega\vec{A} - j\omega\nabla v. \tag{7}$$

The weak Galerkin form, valid for the eddy current region Ω follows:

$$\begin{aligned} &\int_\Omega \nabla \times \vec{N}_i \cdot \frac{1}{\mu} \nabla \times \vec{A}\, d\Omega + \int_{\Gamma_H} \vec{N}_i \cdot (\vec{n} \times (\frac{1}{\mu} \nabla \times \vec{A}))\, d\Gamma \\ + &\int_\Omega \vec{N}_i \cdot j\omega\sigma(\vec{A} + \nabla v)\, d\Omega = 0 \\ &\int_\Omega N_i \nabla \cdot (j\omega\sigma(\vec{A} + \nabla v))\, d\Omega = 0. \end{aligned} \tag{8}$$

The introduction of the magnetic scalar Φ

$$\vec{H} = \vec{H}_s - \nabla\Phi \tag{9}$$

with $\vec{H}_s$ representing the impressed coil field leads to the differential equation for the air region Ω_a:

$$\int_{\Omega_a} N_i\, \mu \nabla\Phi\, d\Omega = \int_{\Omega_a} N_i\, \mu\vec{H}_s\, d\Omega. \tag{10}$$

V. Probe arrangement and investigation setup

Fig. 7 shows a saddle shaped coil with a conducting object immersed in the center region. Above the metallic specimen a GMR-sensor is placed so that its axis of sensibility is radially directed. In this work, the measurements have been carried out at two different sized specimen. Type A is sized by $20 \times 10 \times 2$ mm, whereas type B possesses the dimensions $20 \times 5 \times 2$ mm. Both specimen are made of copper. Line 1 indicates the movement of the specimen along the centerline of the pair of saddle shaped coils, whereas the displacement along the x-axis is drawn as line 2.

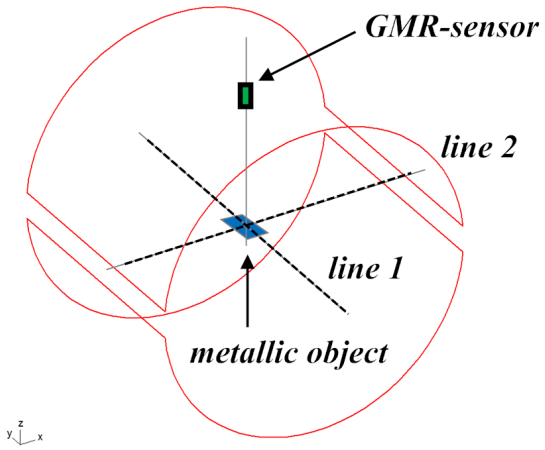

Fig. 7. Arrangement of coils, metallic specimen and GMR-sensor.

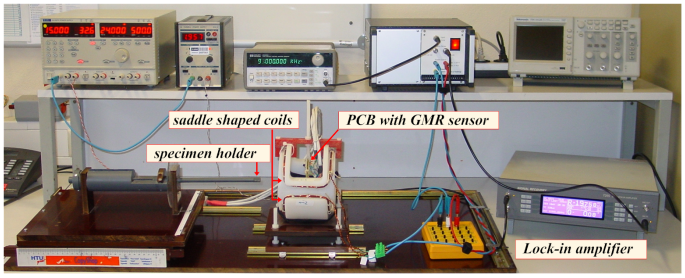

Fig. 8. Photo shot of the measurement setup, essential equipment indicated.

For all measurements, the previously explained lock-in amplifier has been used and $N = 5$ repetitions for the signal averaging have been carried out. At first, the specimen A has been moved along the y-axis. Fig. 9 shows the lapse of the averaged values. Thereby, y-intervalls of 5 mm have been chosen. Without doing to much statistics, the minimum and the maximum at each y-position is plotted by the bars, too. This represents the confidence level for the measurements.

The averaged values of Fig. 10 have been compared with the solutions of Finite Element (FE) computations and are drawn in Fig. 10.

When postprocessing the FE-solutions, the radial component of the magnetic field density $\vec{B}$ at the GMR sensor position is available. All the numerically obtained values have been scaled, so that the minimum of the curve corresponds with the measured minimum. Doing so, the solutions become

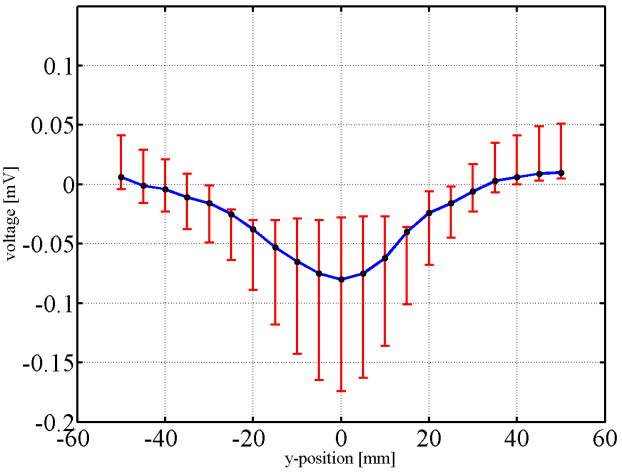

Fig. 9. Measurements averaged with confidence level, $N = 5$, displacement along line 1, specimen type A.

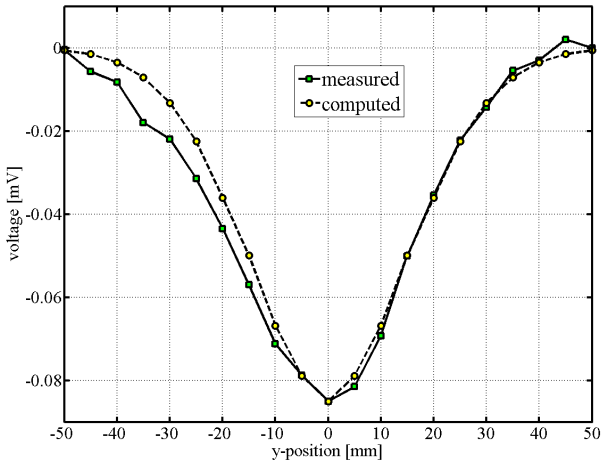

Fig. 10. Measured and computed results in comparison, displacement along line 1, specimen type A.

comparable. A satisfactory agreement with the measurements can be stated.

As can be seen in Fig. 11, also for the specimen type B, where the eddy current region becomes much smaller, a sharp contur has been obtained. The slight deviation to the computed results on the left slope points to the displacement procedure not running exactly y-axis aligned.

Before the lines shown in Fig. 12 have been taken, the small specimen of type B has been rotated by 90° along the y-axis (cf. Fig. 7). Within this position the eddy currents induced in the specimen become much more smaller. Nevertheless, a very distinctive characteristic could be measured.

The displacement of specimen type B along the x-axis leads to a distinguish devolution of the measurements, as well (Fig. 13). All together, satisfying measurements could be taken. The temperature drift of the current source, biasing the GMR sensor has been turned out to have the most crucial influence on the quality of measurements. Therefore a temperature

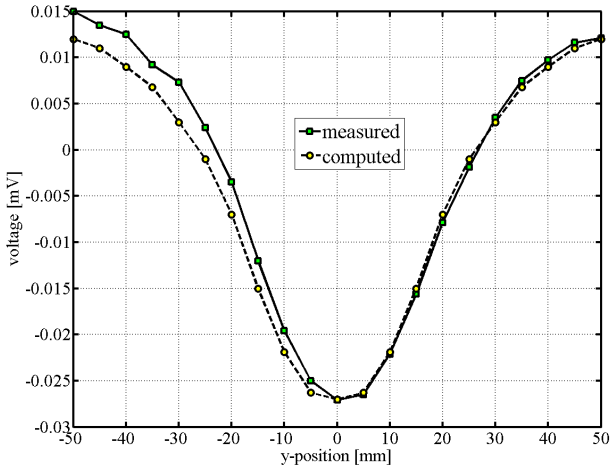

Fig. 11. Measured and computed results in comparison, displacement along line 1, specimen type B.

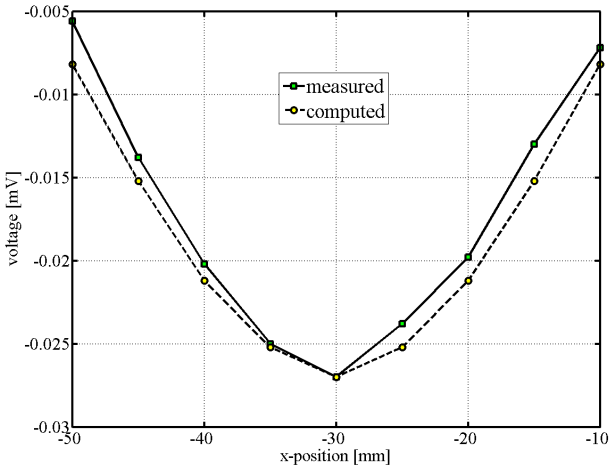

Fig. 13. Measured and computed results in comparison, displacement along line 2, specimen type B.

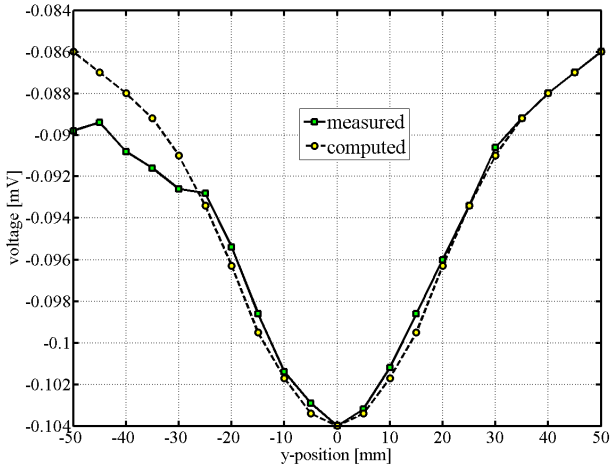

Fig. 12. Measured and computed results in comparison, displacement along line 1, specimen type B, 90° vertically rotated.

stabilized type of current source had to be employed.

VI. Conclusion

On a canonical eddy current problem the proposed localization method has been investigated. Thereby, a GMR-sensor gave answers about the reaction field. In order to reduce the signal to noise ratio, a lock-in amplifier has been used and simultaneously a signal averaging procedure has been carried out. The achievable accuracy of the measurements has been shown by comparisons to Finite Element computations. Based on the sufficiently good agreement for all configurations measured, the reliability of the measurements can be stated and the feasibility of the method suggested has been demonstrated.

Certainly, higher sophisticated measurement setup methods may improve the accuracy of the measurements further. A possible ansatz can lie in biasing the GMR sensor with an AC signal of the same frequency as the excitation current but 180° phase shifted to it. In this case, the output voltage of the sensor can be compensated to zero when no specimen is present. But this can be a topic for continuative investigations. The use of gradiometric GMR sensors may improve the noise situation, as well.

References

[Jen-Tzong *et al.* (2006)] Jen-Tzong Jenga, Guan-Shiun Lee, Wen-Chu Liao, Chia-Lun Shu, "Depth-resolved eddy-current detection with GMR magnetometer", *Journal of Magnetism and Magnetic Materials*, 304 (2006) pp. e470 - e473, DOI:10.1016/j.jmmm.2006.02.070.

[Bíró (1999)] O. Bíró, "Edge element formulations of eddy current problems", *Comput. Methods Appl. Mech. Engrg.*, 169 (1999) pp. 391 - 405.

[Thomson (1856-1857)] W. Thomson, "On the Electro-Dynamic Qualities of Metals: Effects of Magnetization on the Electric Conductivity of Nickel and of Iron", *Proceedings of the Royal Society of London*, 8, pp. 546-550, (1856-1857).

[Nobel (2007)] "The Discovery of Giant Magnetoresistance", compiled by the *Class for Physics of the Royal Swedish Academy of Sciences*, 9, October 2007, www.kva.se

[Howson *et al.* (1999)] M.A. Hawson et. al., "Magnetic multilayers of Fe/Au: role of the electron mean free path", *Journal of Physics*, Condens. Matter 11, pp. 5717-5722, (1999), http://iopscience.iop.org/0953-8984/11/30/304.

[Nor *et al.*] A.F.Md. Nor, E.W. Hill, K. Birthwistle, M.R. Parker, "Noise in NiFeCo/Cu spin valve sensors", *Sensors and Actuators*, (81), Elsevier, pp. 67-70, (2000), PII: S0924-4247(99)00120-X

[Jury *et al.* (2002)] J.C. Jury et. al., "Measurement and Analysis of Noise Sources in Giant Magnetoresistive Sensors Up to 6 GHz", *IEEE Trans. on Magn.*, Vol 38, No. 5, pp. 3545-3555, (2002).

[Fermon *et al.* (2005)] C. Fermon, M. Pannetier-Lecoeur, N. Biziere, B. Cousin, "Optimized GMR sensors for low and high frequencies applications", *Sensors and Actuators*, A 129, pp. 203-206, DOI:101016/j.sna.2005.11.043.

[Kraftmaker (2010)] Y. Kraftmaker, "Noise reduction by signal accumulation"', *Phys. Teach.*, Vol. 44 (2006), pp. 528 - 530.

[Umer and Sabieh (2006)] H. Umer and M.A. Sabieh, "Reducing noise by repetition: introduction to signal averaging", *Eur. J. Phys.*, 31 (2010), pp. 453 - 465, DOI:10.1088/0143-0807/31/3/003.